N89-20082

VISUAL PERCEPTION AND GRASPING FOR THE EXTRAVEHICULAR ACTIVITY ROBOT

Final Report

NASA/ASEE Summer Faculty Fellowship Program--1988

Johnson Space Center

Prepared By:	Scott A. Starks, Ph.D.
Academic Rank:	Professor
University & Department:	East Texas State University Computer Science Commerce, Texas 75428
NASA/JSC	
Directorate:	Engineering
Division:	Systems Development & Simulation
Branch:	Intelligent Systems
JSC Colleague:	Kenneth R. Crouse, Ph.D.
Date Submitted:	August 17, 1988
Contract Number:	NGT 44-005-803

ABSTRACT

Automation and robotics have played important roles in space activities for many years, most notably in planetary exploration and Space Shuttle operations. There are several major robotic systems being designed and developed for the Space Station. One such system is the Extravehicular Activity Retriever (EVAR). The EVAR will be an intelligent free-flying robot which will have the ability to locate, track, maneuver to, and retrieve objects which have been detached from the Space Station. Most notably, the EVAR is being designed so that it will be able to retrieve crew members who have become stranded during extravehicular activity. The EVAR is undergoing a series of ground-based demonstrations in the precision air bearing floor facility located at the NASA Johnson Space Center. These tests serve as a means of providing proof of concept as well as demonstrating system level performance of the EVAR hardware and software.

Space-based robotics systems are presented with many technical problems which can be avoided in robots designed for terrestrial settings. Due to the near absense of gravity in space, the manipulation of objects is quite different from what is normally experienced on earth. In contrast to the structured environments in which factory robots operate, space-based robots must deal with environments containing a high degree of uncertainty. The harsh nature of lighting in space creates visual perception problems as well. The end result is that although many robots have been developed which perform adequately on earth, much technology remains to be developed to support intelligent space-based robots such as the EVAR.

This study considers one such area of technology, the development of an approach to the visual perception of object surface information using laser range data in support of robotic grasping. This is a very important problem area in that a robot such as the EVAR must be able to formulate a grasping strategy on the basis of its knowledge of the surface structure of the object. This paper presents a description of the problem domain and formulates an algorithm which derives an object surface description adequate to support robotic grasping. The algorithm is based upon concepts of differential geometry namely, gaussian and mean curvature.

INTRODUCTION

It is the purpose of this paper to formulate an algorithm for the calculation of surface shape and structure from laser range data. This algorithm was developed with the intent of using it to assist in the closed loop control of the grasping operation performed by the Extravehicular Activity Retriever (EVAR). In order to perform the grasping operation a robot such as the EVAR must have knowledge of the structure of the surface of the object to be grasped. Using such information, the robot can plan the reach of its manipulator to the object and can preshape its hand in such a way so as to accommodate the object and ensure a stable grasp. The algorithm calculates information about the surface structure and is based upon concepts from differential geometry, namely the gaussian and mean curvatures of a surface. The approach to be presented is based in part upon previous works by other investigators [1], [2].

This report is based upon preliminary results from a study initiated this summer at the Johnson Space Center. In addition to the presentation of the algorithm for curvature-based surface calculation, this report also describes some of the key criteria relating to the determination of grasping strategies. It also presents a framework which allows a robot to store essential surface characterization and grasp configuration information in a computerized library. Under such a framework, a robot can make use of previously generated knowledge about objects and hand configurations to simplify the complexity of grasp planning.

EXTRAVEHICULAR ACTIVITY RETRIEVER

The use of robots in hazardous environments such as space is rapidly expanding. Numerous studies and symposia have been conducted on this very important topic [3]. The EVAR is a voice-supervised, intelligent, free-flying robot which is currently being designed, developed, and demonstrated in a ground-based laboratory facility at the Johnson Space Center [4]. When operational, the EVAR will be used to retrieve objects such as construction materials, equipment, and tools which have been accidentally separated from the Space Station. The EVAR will be in a stand-by mode whenever astronauts perform extravehicular activity (EVA). If an astronaut becomes detached from the Station, the EVAR will be summoned to locate, fly to, grapple and return the astronaut to the Station. The EVAR is being designed so that it can accommodate an unconscious or uncooperative astronaut.

The EVAR consists of six integrated subsystems: the Manned Maneuvering Unit (MMU), two robotic arms with grippers, a video and tracking system, a 3D laser imaging system, an onboard computer system, and a data and control network. The MMU provides the EVAR with the ability to fly about in a manner similar to that of an astronaut during EVA. The two robotic arms are anthropomorphic in nature. One of the grippers is a dexterous hand while the other is a parallel jaw gripper. The EVAR video and tracking system employs two black and white cameras, a tracking system, and a monitor to allow for backup supervisory control of EVAR operations by personnel at a remote location. One camera enables target acquisition and tracking, while the second can be used to assist during target grappling. The 3D laser imaging system is an Odetics 3D laser radar ranger. This subsystem, often called a 3D mapper, consists of a scan unit, an electronics unit, and a power supply. The 3D mapper provides direct digital range measurement and is capable of scanning a 60 degree horizontal by 60 degree vertical area with a 128X128 raster scan.

The frame rate of the system is every .835 seconds. The onboard computer system consists of several transputers and other processors. The data and control network enables the routing of communication and control information among the various subsystems of the EVAR. A three phase ground demonstration program for the EVAR has been planned and scheduled. The first phase of the program was successfully completed this past year. The second milestone demonstration will be conducted this fall at the precision air-bearing floor facility at NASA Johnson Space Center.

ROBOTIC GRASPING

Robot manipulation is a complex process that consists of several steps: sensing, task planning, trajectory planning, grasping, and path following. With respect to grasping, there are three principal grasp selection criteria which are of major concern. They are described briefly below.

Safety. The criteria of safety involves the issue of damage control as applied to three areas: (i) the target object must be safe in the sense that there should not be any damage to the object during the grasp operation; (ii) the robot must avoid damaging itself as it performs the operation; and (iii) the task environment should remain damage-free during the operation. Whereas the EVAR is being developed to retrieve stranded crew members and possibly very expensive Space Station construction tools and materials, requirement (i) is an overriding concern in the development of grasping strategies for the EVAR. In addition, the EVAR itself will be an expensive piece of equipment, therefore elevating the importance of requirement (ii).

Reachability. This criteria centers on the ability of the hand to reach a particular target. In other words, there must be a sufficiently large workspace to accommodate the movement of the hand during the operation. This requires that the hand be able to reach the object at some initial hand configuration and, with the object in hand, to follow a collision-free path to a final location. In addition, the workspace of the hand's fingers must be large enough relative to the size of the object for the fingers to secure the proper grasp.

Stability. The grasp must be stable in the presence of external forces which could be exerted on the grasped object of the hand during the manipulation process. By stable, we simply mean that a grasp does not permit the target to move or slip with respect to the hand.

It is clear that the above grasp criteria are closely related to the characteristics of the targets and the environments which they occupy. In fact, they form the bases upon which grasp configurations and operation strategies are determined. In the following section, the characteristics of targets which are most critical to the grasping operation are presented.

CHARACTERISTICS OF OBJECTS

Objects can be characterized by three different types of attributes (geometric, physical, and mechanical) [5]. Geometric attributes include the size of an object, the shape of the object, and the shape of the contact surface. With regard to grasping, the size of the object is most important in determining the accessibility of the object. The shape of the object as well as that of its contact surface influence grasp stability and hand preshaping. Prior to selecting a grasp, a list of candidate grasp configurations can be extracted from a library. Candidate grasp configurations can then be evaluated on the basis of the geometric attributes of the object. The set of candidate grasp configurations could then be narrowed by removing those grasp configurations that would lead to unstable grasps. Finally, the physical and mechanical characteristics of the object could be taken into consideration.

Physical attributes include the mass, mass distribution, and inertia of the objects. The

center of mass affects the stability of the grasp configurations. The physical attributes of the target are difficult, if not impossible, to extract using solely non-contact methods of sensing, such as imaging or laser ranging. This being the case, it would be advantageous to develop a library containing the physical properties of objects likely to be retrieved by the EVAR [6]. By classifying the target, the EVAR could then retrieve its physical attributes and make use of these in the formulation of a grasp strategy.

Target objects can be grouped into five categories based upon mechanical attributes. These categories are rigid, brittle, elastic, flexibile, and slippery objects. Rigid objects exhibit a high degree of stiffness which makes them unlikely to deform during grasping. Unlike rigid objects, brittle objects have low stiffness. Potentially, objects of this type can be very fragile and thus easily damaged. Grasping brittle objects requires accurate information concerning the shape and size of contact areas in that they can be easily damaged. Elastic objects are characterized on the basis of behavior of their surfaces about the point of contact by a manipulator. When a force is exerted on an elastic object, deformation of the surface at the point of contact of the manipulator may appear. When the force is removed, the deformation disappears, restoring the object to its original form. Elastic objects are typically the easiest objects to grasp. Unlike elastic objects, flexible objects have low stiffness. As a result, deformation which result from the application of a force remain subsequent to the removal of the force. Normally, detailed shape information about the target is not as important for grasping elastic objects. Large contact areas are essential for grasping flexible objects. Slippery objects are perhaps the most difficult to grasp and handle. Whereas the coefficient of friction at the contact area is very low, the stability of the grasp can be diminished.

It is important to note that the mechanical attributes of objects should be considered in conjunction with geometric and physical attributes in the determination of grasp strategies. Such design ensures that any drawback in one aspect can be compensated by advantages offered by the others.

VISUAL PERCEPTION OF RANGE IMAGING

In a broad sense, visual perception of range images can be viewed as the process of interpreting measurements made using any of a variety of range sensors. Because the success of automated devices depends critically on systems with the ability to sense and understand the environment, range image perception has received the attention of many investigators. Automatic systems have been designed to work in tightly structured environments such as assembly lines in factories. Unfortunately, much of the technology associated with systems of this type is not directly transferrable to the EVAR in that the EVAR must have the ability to cope with uncertainities in its environment.

The EVAR is equipped with a laser ranging device which is capable of determining a range image of the environment surrounding the robot. A range image is merely a large collection of distance measurements from a known reference coordinate system to surface points on objects within a scene. If the distance measurements in a range image are listed relative to three orthogonal coordinate axes, the range image is said to be in *xyz* form. If the distance measurements indicate range along 3D direction vectors indexed by two integers (i, j), the range image is said to be in r_{ij} form. Any image in r_{ij} form can be converted directly to *xyz* form, but the converse is not true [7]. The term image is used because any r_{ij} range image can be displayed on a video monitor, and it is identical in form to a digitized video image from a television camera. In addition the term visual perception is often associated with the extraction of information from a range image for the same reason.

Range images can be a source of valuable information for an automated machine. The EVAR can use range image information to determine the location and orientation of objects in its environment. This information can be used to plan the EVAR's movements and actions. Surface fitting techniques make use of range data to produce a geometric description of objects. In this report, we are interested in determining the underlying surface structure of targets which the EVAR will be responsible for grasping. An approach to extracting the surface structure of a target is critical to the grasp operation because manipulators grasp surfaces. The following section presents an approach to surface fitting which is based upon curvature concepts taken from the field of differential geometry.

SURFACE FITTING

The surface fitting problem can be stated as follows: given three m x n arrays of x, y, and z coordinates, we would like to determine a surface that approximates the data in the least-squares sense and that is smooth. In a mathematical sense, smoothness is defined as the twice-differentiability of the surface at all points. Fitting a surface to an L x L window of data is equivalent to computing a surface fit for a roughly rectangular grid of data values. Intuitively, a roughly rectangular grid is one that has been obtained from a rectangular mesh that has been deformed to fit the surface. We may represent the surface in parametric form by the three equations

$$x = f(s,t),$$

$$y = g(s,t),$$

$$z = h(s,t),$$

where s and t are the parameters, and the functions f, g, and h are tensor products of splines in tension. The fitting can be viewed as a mapping from 2D space to 3D space. The 2D space is characterized by the parameters s and t and the 3D space is the standard cartesian space.

Principal curvatures at a point on a surface indicate how fast the surface is pulling away from its tangent plane at that point. Principal curvatures can be computed by estimating partial derivative infomation for the surface. The principal curvatures will achieve a local maximum in the area surrounding a discontinuity in the surface, for example an edge in the object. By thresholding the values of the principal curvatures, we can declare the edge points in a range image.

When a plane passing through the normal to the surface at a point P is rotated about this normal, the radius of curvature changes and will be a maximum distance r_1 for a definite normal section s_1 and a minimum r_2 for another normal section s_2. The reciprocals $k_1 = 1/r_1$ and $k_2 = 1/r_2$ are called the principal curvatures; the directions of the tangents to s_1 and s_2 at P are called the principal directions of the surface at P. Gaussian curvature at point P is defined as the product of the two principal curvatures. It can be proven that the gaussian curvature depends only upon the coefficients of the first fundamental form of a surface and their derivatives. The coefficients of the second fundamental form share the previously stated property. The first and second fundamental coefficients also determine the surface uniquely up to a rigid body transformation. As a

result, the gaussian curvature is said to be an intrinsic property of the surface. The principal curvatures at a point on a surface can be computed in terms of the parameters s and t using the following approach. Let $\mathbf{X}(s,t)$ represent the surface

$$\mathbf{X}(s,t) = [\, x(s,t),\, y(s,t),\, z(s,t)\,]^T.$$

Here, bold face notation is used to denote a vector quantity. If we let partial differentiation be represented by subscripts, the differential element $d\mathbf{X}$ is a vector given by the relationship

$$d\mathbf{X} = \mathbf{X}_s\, ds + \mathbf{X}_t\, dt,$$

where

$$\mathbf{X}_s = d\mathbf{X}/ds = [\, x_s,\, y_s,\, z_s\,]^T,$$

$$\mathbf{X}_t = d\mathbf{X}/dt = [\, x_t,\, y_t,\, z_t\,]^T.$$

If we take the scalar product of $d\mathbf{X}$ with itself we obtain a relationship which is known as the First Fundamental Form of the surface, I, which is given below:

$$I = d\mathbf{X} \cdot d\mathbf{X} = (\, \mathbf{X}_s\, ds + \mathbf{X}_t\, dt\,) \cdot (\, \mathbf{X}_s\, ds + \mathbf{X}_t\, dt\,)$$

$$= E\, ds^2 + 2F\, dsdt + G dt^2,$$

where the First Fundamental Coefficients (E, F, and G) are given by:

$$E = |\, \mathbf{X}_s\,|^2 = x_s^2 + y_s^2 + z_s^2,$$

$$F = \mathbf{X}_s \cdot \mathbf{X}_t = x_s\, x_t + y_s\, y_t + z_s\, z_t,$$

$$G = |\, \mathbf{X}_t\,|^2 = x_t^2 + y_t^2 + z_t^2.$$

The unit normal is then given by

$$\mathbf{N} = (\, \mathbf{X}_s \times \mathbf{X}_t\,) / |\, \mathbf{X}_s \times \mathbf{X}_t\,|.$$

The differential of the unit normal is

$$d\mathbf{N} = \mathbf{N}_s\, ds + \mathbf{N}_t\, dt.$$

If we take the negative of the scalar product of the differentials of the surface and the unit normal, we obtain the Second Fundamental Form for the Surface,

$$II = -d\mathbf{X} \cdot d\mathbf{N} = -\,(\mathbf{X}_s\, ds + \mathbf{X}_t\, dt) \cdot (\mathbf{N}_s\, ds + \mathbf{N}_t\, dt) =$$

$$= L\, ds^2 + 2\, M\, ds\, dt + N\, dt^2,$$

where the Second Fundamental Coefficients (L, M, and N) are given by:

$$L = -X_s \bullet N_s,$$

$$M = -1/2 \, (X_s \, . \, N_t + X_t \, . \, N_s),$$

$$N = - X_t \bullet N_t.$$

The gaussian curvature K at any point on the surface is defined as the product of the two principal curvatures k_1 and k_2 and can be expressed in terms of the First and Second Fundamental Coefficients as

$$K = k_1 k_2 = (LN - M^2) / (EG - F^2).$$

The mean curvature H is given by the average of the two principal curvatures. It may be expressed in terms of the First and Second Fundamental Coefficients as well,

$$H = (LG - 2MF + NE) / (2(EG-F^2)).$$

The principal curvatures are given by,

$$k_1 = H - SQRT(H^2 - K),$$

$$k_2 = H + SQRT(H^2 - K).$$

The above formulas can be used to compute the gaussian and mean curvatures. Let us assume that the gaussian and mean curvatures for a particular point referenced by the indices (i, j) in a range image have been calculated and are stored in arrays $K(i, j)$ and $H(i, j)$ respectively. The points on a surface can then be classified according to the signs of these quantities: positive, negative, or zero. It turns out that there are only eight possible outcomes for surface characterization based upon the signs of the gaussian and mean curvatures. We introduce notation for two functions (modified signum function and the surface classification function). The modified signum function is a mapping of a scalar argument into one of three values (1 , 0 , or -1). For positive e, it is defined as:

$$\begin{aligned} sgn_e (y) = \; & 1 \text{ if } y > e \\ & 0 \text{ if } |y| < e \\ & -1 \text{ if } y < -e . \end{aligned}$$

We take advantage of the clarity afforded by use of the modified signum function to introduce the surface classification function

$$T(i,j) = 1 + 3\,(1 + \mathrm{sgn}_{e1}(H(i,j))) + (1 - \mathrm{sgn}_{e2}(K(i,j))).$$

The positive scalars *e1* and *e2* are chosen to be close to zero. They enable the mapping to zero of a number within the limits of the numerical accuracy of the machine and the algorithm. Figure 1a gives the mapping of the values of the modified signum function applied to the gaussian and mean curvatures. Figure 1b gives a pictorial interpretation of the eight possible surface classifications afforded by the function T(i, j).

CURVATURE-BASED SURFACE CALCULATION ALGORITHM

This section presents an algorithm to compute the object description in terms of jump boundaries, internal edges, and regions homogeneous in the sign of their gaussian and mean curvatures. The algorithm can be summarize as a sequence of the following steps:

- Divide the range image into overlapping windows.
- Detect jump boundaries and fit patches to windows of data not containing jump boundaries.
- Compute the principal curvatures and extract edge points.
- Classify each nonedge point in a patch as one of the eight possible surface classifications presented previously.
- Group all points of the same type in a patch and its neighboring patches into a region.

The details of each step in the algorithm are as follows. In the first step, the division of the input arrays of (x, y, z) coordinates into L x L windows should be overlapped to ensure that an internal edge is always contained in a patch.

In the second step, the relative degree of scatter exhibited by the data is reflected in the standard deviation of the euclidean distance between adjacent data points within the L x L window. In the vicinity of a jump boundary of an object, the standard deviation of these euclidean distances will be relatively high. Jump boundaries can be detected by means of a threshold test. After the jump boundaries have been detected, smooth patches based upon 2D B-splines can be fitted to the data in the window not containing a jump discontinuity [8]. In the presence of a jump boundary, the window size can be modified to ensure that the window excludes the jump boundary. In order to detect fine detail in the scene it is important that the size of the objects be much larger than the size of the L x L window.

In the third step of the algorithm, we attempt to detect all those points that belong to or fall on internal edges of the object. As was mentioned previously, in the vicinity of an edge, the values for the principal curvatures will be high and in fact achieve a local maximum. As a result, we first determine all points exhibiting principal curvatures above threshold. Due to the presence of noise in the data and an inappropriate choice of thresholds, clusters of edge points may appear in the vicinity of a true edge position. To eliminate these clusters of computed edge points, a suppression of nonmaxima is applied at every edge point. That is, we only declare an edge to be present at points where the curvature is a local maximum. Nonmaxima suppression is applied in a direction perpendicular to the edge directions which is the direction associatated with the maximum absolute principal curvature.

The next step is to group object points into homogeneous regions. All points in a

T(i,j)	Surface Type
1	Peak
2	Ridge
3	Saddle Ridge
4	Not possible
5	Flat
6	Minimal
7	Pit
8	Valley
9	Saddle Valley

Figure 1a. Classification of surfaces

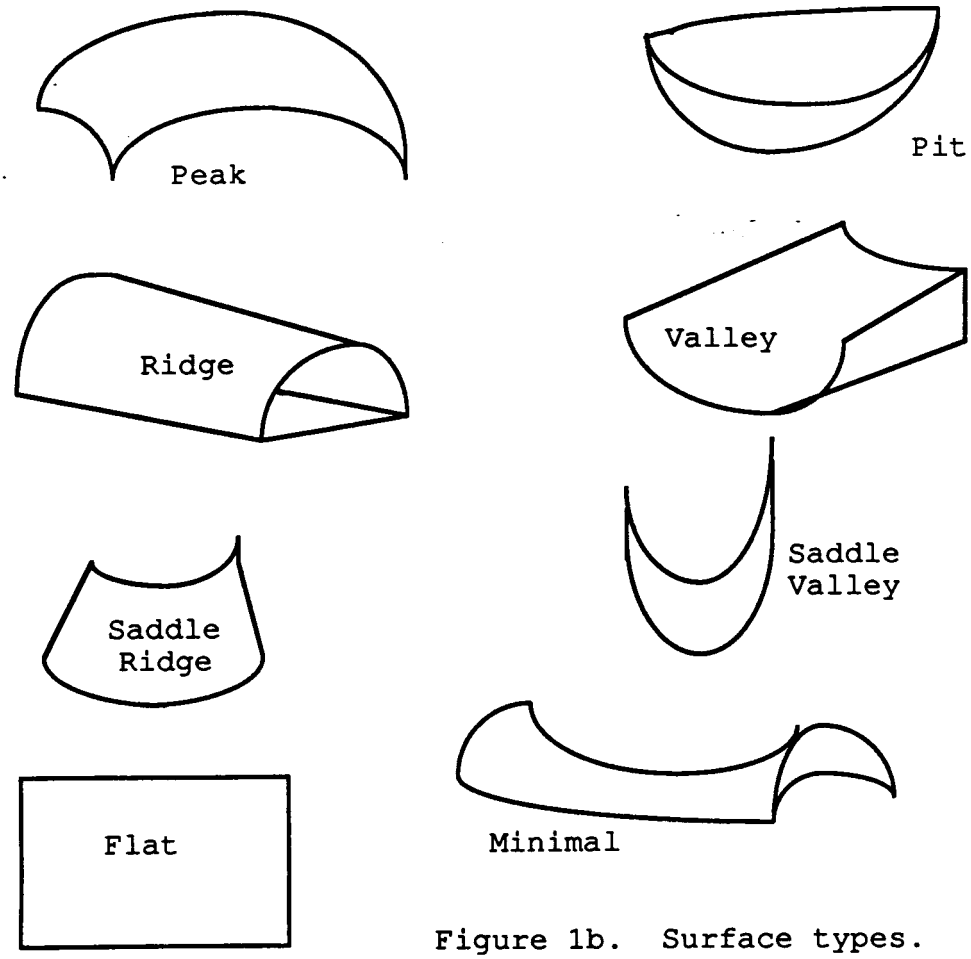

Figure 1b. Surface types.

patch are classified into one of the types indicated in Figure 1b. All points of the same type are grouped together into a larger region. Ther merging of points does not require explicit fitting of a new surface to this homogeneous region since the surfaces are chosen to be smooth. Each homogeneous region is assigned a label depicting its type. Internal edges may occur within regions. The extent of regions can be delineated by jump boundaries, internal edges, and curvature edges, which we define as places where there is a change in curvature-based classification.

The object representation in terms of regions and curvature-based properties , as described above, have the following advantages:

- it is invariant under transformation of independent parameters of the surface.
- it is invariant to rigid body transformation and is therefore independent of viewpoint.

EVAR GRASPING

Operational constraints of the EVAR Demonstration Program demand that grasping be performed in a real-time, closed-loop manner. Under Phase II of the program, both video and range data will be available for the demonstration. In addition, the target will be a stationary object. It is assumed that the EVAR hand will be in close proximity (within a foot) of the target prior to grasping.

Probably the single most important property of the human hand is its ability to grasp a wide range of objects. The incorporation of a hand on the EVAR will enable the EVAR to grasp a wide variety of objects as well. Grasping involves the coordination of many degrees of freedom. In an automated system, we wish to reduce the number of degrees of freedom associated with robotic grasping. One approach to achieve this goal is based upon the notion of classification of grasp configurations. By dealing with grasp configurations in a packaged format through classification, one can simplify the amount of planning associated with the grasping operation [9]. This approach is based upon the abilty of the automated system to recognize surface structures based upon features derived from image and range measurements. Features could be constructed using the curvature-based surface representation calculation algorithm to describe the underlying suface structure of the object to be grasped. These features could be matched against those stored in a surface/grasp library [10]. This library would contain grasp configuration which would relate to the particular surface structure. In addition, the library would contain the physical and mechanical attributes of the associated object. Suppose the EVAR is presented with a surface structure similar to one previously encountered and successfully grasped. Under such circumstances, the EVAR can make use of information previously generated concerning grasping to sieze the target. This information would consist of hand preshape geometry, grasp approach, and other relevant information.

If the surface cannot be classified by matching its surface features with those contained in the surface/grasp library, it will be necessary to formulate a new grasp strategy. In that the hand must grasp surfaces, the information generated using the algorithm would be useful in the development of a new grasp configuration. If a new configuration is developed and successfully used to produce a stable grasp, then it is stored along with the underlying target surface structure in the surface/grasp library. Needless to say, the surface/grasp library will be dynamic. As new objects are successfully grasped, the library will expand. The overall approach is illustrated in Figure 2.

SUMMARY

This paper has presented an algorithm for the calculation of curvature-based surface

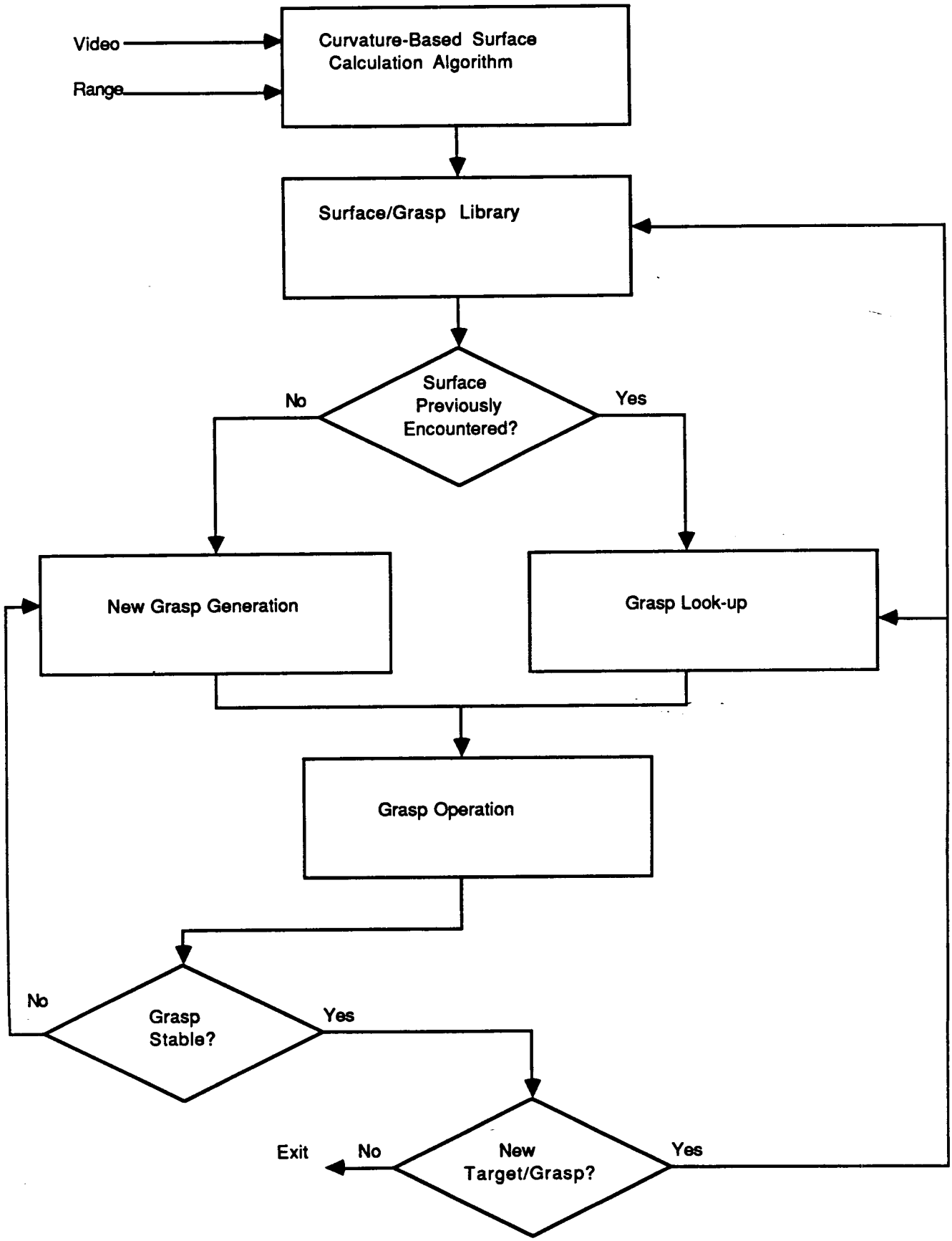

Figure 2. Framework for grasp operation.

characteristics for objects using range data. At the present time, this algorithm is being implemented in the programming language C. Although the approach to surface description based upon curvature concepts taken from differential geometry appears promising, it would be presumptuous to leave the reader with the impression that it will provide all the information necessary for secure and stable grasping for the EVAR. It is essential to integrate this prototype software, when available, in a real-time systems level demonstration in order to fully evaluate its merits. Such a demonstration would bring to light any deficiencies which could then be addressed by future refinements.

REFERENCES

1. B.C. Vemuri, A. Mitiche, and J.K. Aggarwal, "Curvature-based representation of objects from range data," *Image and Vision Comput.*, vol. 4, no. 2, pp. 107-114, May 1986.

2. P.J. Besl and R.C. Jain, "Segmentation through variable-order surface fitting," *IEEE Trans. on Pattern Anal. Machine Intell.*, vol. 10, no. 2, March 1988.

3. J. Erickson, "Manned spacecraft automation and robotics," *Proc. of the IEEE*, vol. 75, no. 3, March 1987.

4. G.J. Reuter, C.W. Hess, D.E. Rhoades, L.W. McFadin, K.J. Healey, and J.D. Erickson, "An intelligent, free-flying robot," to appear in *Proc. of SPIE: Space Station Automation IV*, November 1988.

5. G. Wang and H.E. Stephanou, "Chopstick manipulation with an articulated hand: a qualitative analysis," *Proc. of 1988 IEEE Intl. Conf. on Robotics and Automation*, pp. 94-102, 1988.

6. W.C. Chiou and S.A. Starks, "An introduction to the concept of robot factors and its application to space station automation," *Proc. of SPIE: Space Station Automation*, vol. 580, pp. 53-57, September 1985.

7. P. J. Besl, "Active, optical range imaging sensors," *Machine Vision and Appl.*, vol. 1, no. 2, pp. 127-152, 1988.

8. W. Tiller, "Rational B-splines for curve and surface representation," *IEEE Comp. Graphics and Appl.*, pp. 61-69, September 1983.

9. D.M. Lyons, "A simple set of grasps for a dextrous hand," *Proc. of 1985 IEEE Intl. Conf. on Robotics and Automation*, pp. 588-593, 1988.

10. K. Rao, G. Medioni, H. Lui, and G.A. Bekey, "Robot hand-eye coordination: shape description and grasping," *Proc. of 1988 IEEE Intl. Conf. on Robotics and Automation*, pp. 407-411, 1988.